DOC2B and Munc13-1 Differentially Regulate Neuronal Network Activity

Ayal Lavi[1,2], Anton Sheinin[1,2], Ronit Shapira[1], Daniel Zelmanoff[1] and Uri Ashery[1,2]

[1]Department of Neurobiology, The George S. Wise Faculty of Life Sciences, Tel Aviv University, Tel Aviv 69978, Israel
[2]Sagol School of Neuroscience, Tel Aviv University, Tel Aviv 69978, Israel

Address correspondence to Uri Ashery, Department of Neurobiology, The George S. Wise Faculty of Life Sciences; Sagol School of Neuroscience, Tel Aviv University, Tel Aviv 69978, Israel. Email: uriashery@gmail.com.

Alterations in the levels of synaptic proteins affect synaptic transmission and synaptic plasticity. However, the precise effects on neuronal network activity are still enigmatic. Here, we utilized microelectrode array (MEA) to elucidate how manipulation of the presynaptic release process affects the activity of neuronal networks. By combining pharmacological tools and genetic manipulation of synaptic proteins, we show that overexpression of DOC2B and Munc13-1, proteins known to promote vesicular maturation and release, elicits opposite effects on the activity of the neuronal network. Although both cause an increase in the overall number of spikes, the distribution of spikes is different. While DOC2B enhances, Munc13-1 reduces the firing rate within bursts of spikes throughout the network; however, Munc13-1 increases the rate of network bursts. DOC2B's effects were mimicked by Strontium that elevates asynchronous release but not by a DOC2B mutant that enhances spontaneous release rate. This suggests for the first time that increased asynchronous release on the single-neuron level promotes bursting activity in the network level. This innovative study demonstrates the complementary role of the network level in explaining the physiological relevance of the cellular activity of presynaptic proteins and the transformation of synaptic release manipulation from the neuron to the network level.

Keywords: asynchronous release, genetic manipulation, MEA recording, network burst, presynaptic proteins

Introduction

Understanding the roles of specific proteins in synaptic transmission at the level of single neurons is important, but ultimately, neurons operate together in an ensemble (Brown et al. 1990; Marom and Shahaf 2002; London and Hausser 2005). Neuronal microcircuits are comprised of neuronal networks interacting collectively to produce a functional output (Cobb et al. 1995; Wang and Buzsaki 1996; Hausser et al. 2004; Grillner et al. 2005). Interestingly, small alterations in the firing properties of single neurons can alter the activity of the neuronal circuit (Sharma and Vijayaraghavan 2003; London et al. 2010). However, the contribution of synaptic proteins to neuronal network activity is almost completely unknown. Therefore, understanding the contribution of synaptic proteins to the activity of neuronal networks can elucidate the functional roles of the proteins and of the mechanisms involved in network activity. Specifically, we are interested in discovering how cellular manipulation of the presynaptic proteins DOC2B and Munc13-1 affects the functional properties of the neuronal network.

DOC2B and Munc13-1 are interacting presynaptic proteins which promote vesicle release (Betz et al. 1998; Augustin et al. 1999; Groffen et al. 2006, 2010; Friedrich et al. 2008; Lou et al. 2008; McMahon et al. 2010). DOC2B enhances spontaneous release and its effect depends on submicromolar calcium concentration (Groffen et al. 2010 but see Pang et al. 2011), suggesting that its function depends on the activity of the neuron (Friedrich et al. 2008; Groffen et al. 2010). Furthermore, a recent study demonstrated a role for DOC2B in the regulation of asynchronous neurotransmitter release (Yao et al. 2011) as overexpression of DOC2B in *wt* neuronal cultures specifically increased the slow phase of synaptic release. Munc13-1 enhances vesicle priming and its activity depends on calcium, Calmodulin, and diacylglycerols (Betz et al. 2001; Junge et al. 2004; Lou et al. 2008; Dimova et al. 2009; Shin et al. 2010). As it regulates both Ca^{2+}-evoked and spontaneous release, it has been assumed that it increases the fusion probability of releasable vesicles (Betz et al. 1998; Rhee et al. 2002; Lou et al. 2005, 2008; Basu et al. 2007). Furthermore, the interaction between DOC2 proteins and Munc13-1 in the molecular level might have a positive role in regulating synaptic release (Mochida et al. 1998; Duncan et al. 1999). Thus, DOC2B and Munc13-1 utilize both different and interacting molecular pathways to potentiate presynaptic vesicle release.

A growing body of evidence links between the spontaneous activity in neuronal cultures in vitro and the "up" and "down" states displayed by the neocortex in vivo. Modulation of the oscillation between up and down states during spontaneous activity in vivo has been observed during slow-wave sleep, selective attention, and short-term memory tasks (Goldman-Rakic 1995; Luck et al. 1997; Timofeev et al. 2000; Shu et al. 2003). Therefore, elucidating the principles of spontaneous network activity and its manipulation in the culture might contribution to understanding high-order functions in the behaving animal (Chiappalone et al. 2009; Hinard et al. 2012). Specifically, carefully regulated presynaptic release by synaptic proteins might serve as a general mechanism to tune the synchronization of associated neuronal microcircuits throughout the neocortex.

In this study, we present a novel platform to study the functional role of synaptic proteins in neuronal network activity. We used mouse primary cortical neurons cultured on microelectrode array (MEA) plates to investigate the impact of DOC2B or Munc13-1 overexpression on the spontaneous activity of neuronal networks. These cultures form *ex vivo* neuronal networks which, exhibit recurring patterns of synchronized network-wide spiking activity, often referred to as network bursts (Van Pelt et al. 2004; Eytan and Marom 2006; Wagenaar et al. 2006; Baruchi and Ben-Jacob 2007). Our data demonstrate that Munc13-1 and DOC2B have different effects on the network activity and that by enhancing asynchronous release, DOC2B exerts its properties to increase spiking activity and elevate the synchronization between neurons within network bursts.

Materials and Methods

Neuronal Culturing on Microelectrode Array

Cortical neuronal cultures were prepared from P1 and P2 newborn mice (ICR strain). Cortical tissue was separated from the hippocampus and incubated for 15 min with papain (100 U, Sigma-Aldrich, St. Louis, MO, USA) in Ca^{2+}/Mg^{2+}-free Hank's balanced salt solution (HBSS) (Beit HaEmek, Israel). The tissue was then mechanically dissociated, and the cells were plated in Neurobasal-A (Invitrogen, Carlsbad, CA, USA) supplemented with B-27 (Invitrogen) GlutaMAX-I (Invitrogen), antibiotics (penicillin–streptomycin, Invitrogen), and 5% fetal calf serum to support glia growth on the day of culture preparation. On the following day and twice a week thereafter, medium was exchanged with growth medium, which was similar to the plating medium, but without the serum. The cells were used for substrate-integrated MEA plates (Multi Channel Systems, Reutlingen, Germany) or used for microisland preparation (MEA plates were cultured at one million cells in a 100-µL drop applied to the middle of the plate. Final cell density was estimated at 2500–3000 cells/mm^2). Cultures were kept in an atmosphere of 5% CO_2, 95% air at 37 °C and were recorded 2 weeks after plating (no significant difference in culture age), before and after overexpression of the following proteins: DOC2B separated by an internal ribosome entry sequence (IRES) from enhanced green fluorescent protein (GFP) (DOC2B; 15 cultures), DOC2B^{D218,220N} separated by IRES from GFP (DOC2B^{D218,220N}; 9 cultures), and Munc13-1 conjugated to GFP (Munc13-1; 11 cultures). DOC2B and Munc13-1 recordings were compared to age-matched cultures overexpressing GFP (9 cultures for DOC2B and 12 cultures for Munc13-1). Strontium experiments were performed on naive cultures that were applied with 2 mM Strontium (Sigma) and 4 mM EGTA (Sigma) to replace the existing Ca^{2+} ions in the external solution (Xu-Friedman and Regehr 2000). To allow long-term (hours) recordings before and after virus application, custom-made incubation chambers consisting of a glass cylinder and a plastic ring were glued to MEA plates with Sylgard® 184 (Dow Corning, Midland, MI, USA). The MEA plates used in this study consisted of 60 Ti/Au/TiN+iR electrodes of 30 µm diameter and 500 µm spacing and were pretreated with polyethyleneimine (PEI, 1:5000, Sigma-Aldrich) to promote neuron adhesion.

Molecular and Genetic Manipulations

Protein levels were manipulated by viral overexpression which was carried out by Semliki infectious virions (Ashery et al. 1999) encoding DOC2B-IRES-GFP, DOC2B^{D218,220N}-IRES-GFP (Friedrich et al. 2008), or Munc13-1-GFP virus (Betz et al. 1998). Control virus encoded only GFP. Virus preparation was described by Groffen et al. (2006).

MEA Data Acquisition and Imaging System

The MEA plate was placed in an MEA1060-Inv-BC-Standard amplifier (Multi Channel Systems) with frequency limits of 200–5000 Hz and sampling rate of 10 kHz per electrode. All recordings were performed in growth medium ($[Ca^{2+}] = 1.8$ mM, Invitrogen). While recording, the plate was placed on a heating element embedded in the amplifier to ensure a stable 37 °C temperature. The incubation chamber was covered with a stainless-steel apparatus that delivered the atmosphere from the incubator via silicone tubes and allowed long-term recordings of neuronal network activity. Activity was monitored continuously and spike cutouts were collected and saved to a personal computer via MC Rack software (Multi Channel Systems). The MEA amplifier was mounted on an Olympus IX71 inverted microscope. Time-lapse images were acquired every 15 min with a Retiga SRV digital CCD Camera (QI-imaging, Surrey, BC, Canada) which was controlled by Cell^F imaging software (Olympus). X-Cite fluorescent system delivered UV light to the microscope (X-Cite 120PC Q, Lumen Dynamics Group, Inc., Mississauga, ON, Canada). A simple self-built switch box allowed time-lapse imaging that combined bright-field and fluorescent images.

MEA Data Analysis and Visualization

Acquired data were further processed and analyzed with MATLAB (The Mathworks, Inc.). Spike cutouts of 3 ms triggered with a threshold of 5–7 standard deviations above noise level for each electrode were collected and saved, and the time stamps of each spike cutout were grouped by electrode, and used to identify network bursts. Color-coded raster plots were generated by calculating the average inter-spike interval for each spike (calculated from the average interval of the spike from the following and preceding spike). Network-burst profiles were generated from network-burst raster plots by averaging the firing rate over all the bursts. Hence, the firing rate in the network-burst profiles was also normalized to the number of active electrodes to avoid inter-recording bias (see below and Eytan and Marom 2006). Synchronization was calculated from the average pairwise Pearson correlation for all the electrodes that were active in the network bursts. Synchronization was then standardized by the firing rate and normalized to be comparable between the different conditions. Electrode participation in network bursts was calculated for each recording and from it the "full-blown" network bursts were defined as those in which >50% of the electrodes recorded spiking activity.

Network-Burst Detection

The algorithm was based on user-defined parameters and was similar to that used by Eytan and Marom 2006 (see also Pasquale et al. 2010). Briefly, potential network-burst peaks were identified when the firing rate of the active electrodes in the array crossed a predefined threshold (usually between 1% and 5% of the maximum firing rate in the entire recording; active electrodes were defined as electrodes which recorded an average firing rate >0.02 s^{-1} throughout the entire recording). Next, burst initiation and termination times were identified by defining the maximum allowed interspike interval inside the burst (usually 100 ms). Finally, duplicate bursts, short bursts (by burst duration threshold: 3 ms), weak bursts (by threshold for minimum number of spikes: 6 spikes) and limited bursts (by threshold for minimum number of participating electrodes: 3 electrodes) were removed. Overlapping bursts were united. The burst identification algorithm was based on the above parameters and was slightly adjusted manually to capture all bursts in the recordings and identify "aborted" and full-blown bursts (as described at Eytan and Marom 2006).

Computational Model

A leaky integrate-and-fire postsynaptic neuron was modeled using a custom-written MATLAB script. The model simulated the voltage trace of the postsynaptic neuron as it received excitatory input at various frequencies from 10 presynaptic neurons. Each presynaptic input was transformed into a postsynaptic change in membrane voltage [excitatory postsynaptic potential (EPSP)] with a predefined decay coefficient. The parameters used to model the synaptic input were taken from experimental current-clamp recordings of paired hippocampal neurons (EPSP decay coefficient: 52 ms, EPSP amplitude: 7 mV), and the input frequencies were calculated for every presynaptic neuron from a Poisson distribution (baseline-evoked release frequency: 0.5 ± 0.05 Hz). For each run of the simulation, input frequency was shifted for 5 s from baseline frequency to 0.5, 1, 2, 4, or 5 Hz and afterward shifted back to baseline frequency. Asynchronous release was simulated by changing the presynaptic input synchrony. Increased asynchronous release was modeled as additional presynaptic input events with lower amplitude. The amplitude of the additional asynchronous presynaptic input decayed with an exponential decay coefficient ranging from 10 to 100 ms. Quantitative data for the computational model were taken from the average of 30 independent runs of the simulation for each presynaptic asynchronous decay coefficient.

Microisland Experiments Preparation

Microisland cultures were prepared as follows: Briefly, 0.15% agarose was spread on 18-mm coverslips and allowed to dry. Then, a custom-made stamp was used to apply dots of substrate mixture (0.6 µg rat tail collagen; BD Biosciences, Franklin Lakes, NJ, USA) and 0.3 µg poly-D-lysine (Sigma) in sterile water. Cells were prepared as described above and were plated onto the coverslips (150 000 cells/mL). Under these conditions, the neurons grew on collagen/poly-D-lysine dots and formed networks of 20–100 cells. Two weeks after plating,

the neurons were infected with Semliki Forest virus carrying either GFP or DOC2B-IRES-GFP. Experiments were performed 6–8 h after infection.

Microisland Electrophysiology

The spontaneous excitatory postsynaptic currents (mEPSCs) were measured using a EPC-9 patch clamp amplifier (Heka Instruments, Lambrecht, Germany) and acquired on a Macintosh PPC computer running Pulse Software (Heka Instruments). The bath solution consisted of (in mM): 140 NaCl, 3 KCl, 2 CaCl$_2$, 1 MgCl$_2$, 10 HEPES, 2 mg/mL glucose, pH 7.3–7.4, osmolarity adjusted to 305 mOsm. For mEPSC recordings, the bath solution was supplemented with 1 µM tetrodotoxin (TTX) and 50 µM picrotoxin (PTX). The pipettes were filled with the intracellular solution consisting of (in mM): 135 KCl, 5 glucose, 10 HEPES, pH 7.3, osmolarity 284 mOsm. Holding potential was −60 mV; series resistance compensation was usually kept at 70–80%. Only cells with series resistance of <15 MΩ were analyzed. All analyses were performed utilizing the Igor Pro software package (Wavemetrics, Portland, OR, USA) and custom-written macros. Detection of mEPSCs was based on threshold crossing (6 times standard deviation from baseline noise) and first-derivative algorithm.

Western Blotting

Western blot experiments were performed according to standard procedures. In general, cortical cultures were infected with Semliki Forest virus carrying DOC2B-IRES-GFP (6 cultures) or Munc13-1-GFP (3 cultures) and 7 h later, proteins were extracted by a solubilization buffer. The protein extracts (∼70 µg protein) were run on an SDS-polyacrylamide (12%) gel and then transferred to nitrocellulose membrane by electroblotting. After blocking, the membrane was incubated with the following primary antibodies (incubated in 1% bovine serum albumin with 0.05% azide): rabbit anti-DOC2B (1:500), rabbit anti-Munc13-1 (1:2000), rabbit anti-Synaptotagmin-1 (1:1000), mouse anti-clathrin heavy chain (1:1000), rabbit anti-β-tubulin (1:500), rabbit anti-N-methyl D-aspartate receptor 2B (NR2B; 1:400), rabbit anti-tomosyn (1:2000), mouse anti-glutamate receptor 2 (GluR2; 1:1000), rabbit anti-Munc 18-1 (1:1000), rabbit anti-postsynaptic density-95 (PSD95; 1:1000). Next, the membranes were incubated with the appropriate secondary horseradish peroxidase-conjugated antibody and detection was performed using enhanced chemiluminescence solution (Pierce, Idaho, IL, USA) and exposure to Super RX film (Fujifilm, Tokyo, Japan). DOC2B and Munc13-1 protein quantities were normalized to the quantity of Clathrin heavy chain protein and β-tubulin (respectively), which was not affected by viral overexpression.

Immunocytochemical Staining

Neuronal cultures were plated onto coverslips pretreated with PEI (1:5000, Sigma; 300 000 cells/mL) and maintained at 37 °C in growth medium for 2 weeks, as described above. Cultures were then infected with the DOC2B-IRES-GFP or Munc13-1-GFP-carrying Semliki Forest viruses. Next, cultures were fixed in 4% paraformaldehyde for 45 min, permeabilized with 0.2% Triton X-100 for 5 min and blocked for 1 h in normal goat serum (200 µg/mL), all at RT. Thereafter, cultures were incubated with primary mouse anti-neuronal nuclear protein antibody (NeuN, 1:20, Millipore, Billerica, MA, USA) or primary mouse anti-Glutamate decarboxylase 67 protein antibody (GAD67, 1:1000, Millipore) and labeled with the relevant secondary 568 nm Alexa Fluor® antibody (1:1000, Invitrogen). Finally, all cultures were incubated for 5 min with Hoechst dye to stain cell nuclei and coverslips were mounted on slides. Control stains were as described above but lacked the primary antibodies.

Immunocytochemical Imaging and Analysis

Fluorescent images were acquired with a Nikon DS-Fi1 camera mounted on a Nikon 80i microscope. Images were taken at 20× magnification through FITC, TRITC, and DAPI filters. To subtract nonspecific staining, we used control coverslips, which lacked the primary antibody, and lowered the exposure to minimum. Neuronal infection

efficacy, defined as the percentage of neurons that were infected, was determined from 12 cultures infected with the DOC2B-IRES-GFP Semliki Forest virus and 8 cultures infected with the Munc13-1-GFP Semliki Forest virus. Infection of inhibitory neurons was determined from 11 cultures infected with the DOC2B-IRES-GFP Semliki Forest virus and 8 cultures infected with the Munc13-1-GFP Semliki Forest virus. We analyzed the images with Image-Pro Plus software (Media Cybernetics, Silver Spring, MD, USA) by presetting a threshold for every antibody. All analyses were inspected manually.

Results

Efficient Expression of DOC2B in Microelectrode Array Plates

In order to investigate the role of synaptic proteins in neuronal network activity, we first set up the MEA system with the DOC2B protein (the same method was later applied to Munc13-1). DOC2B is known to regulate both the spontaneous miniature neurotransmitter release (minis) (Groffen et al. 2010; Pang et al. 2011) and the asynchronous phase of synaptic release from single neurons (Yao et al. 2011). To clarify the effect of DOC2B on neuronal networks, we overexpressed DOC2B in high-density cortical mouse neuronal networks (∼2500–3000 cells/mm^2, see Materials and Methods section). Neurons were cultured on MEA plates and recorded after 2 weeks, before and after overexpression of DOC2B-IRES-GFP or the control protein GFP in cultures prepared from the same animals (Fig. 1A). To understand the effect of DOC2B on neuronal networks, we examined its effect on spontaneous network activity. Each MEA plate consisted of 59 recording electrodes, each capable of recording the activity of several neurons (Fig. 1B). Spike cutouts were extracted from each recording electrode by adjusting a predefined threshold and were analyzed with custom-written MATLAB algorithms (see Materials and Methods section). Data were visualized by raster plots, in which each row indicates the activity recorded by a single electrode, and each black bar represents a neuronal spike (Fig. 1B). Typical spontaneous activity consisted of periods of increased network-wide burst activity followed by interburst periods with decreased activity; Figure 1B corresponds to 3 short network bursts (the left one is boxed in dark gray) separated by 2 longer periods of decreased interburst activity.

As we wanted to see a clear network effect and to minimize adaptation processes, we aimed at a fast and efficient expression that would alter DOC2B levels in a large number of neurons collectively. We compared the chemical-based transfection method with 2 virus-based infection systems: the Lentivirus system and the Semliki Forest virus system. Chemical-based transfection proved to be fast but resulted in very low efficiency. On the other hand, the Lentivirus system led to very high infection efficiency but had a lag of 24–48 h, which can result in more significant adaptation processes occurring in the network (Lazarevic et al. 2011). In contrast, the Semliki Forest virus expression system was fast (reaching high expression levels within few hours) and resulted in a homogeneously high infection rate that favored neuronal infection over glial infection and promoted a network-wide effect (Supplementary Fig. S1). To characterize the time course of DOC2B expression in the neuronal network, we quantified the increase in DOC2B expression levels by western blot analysis and compared the results with the time
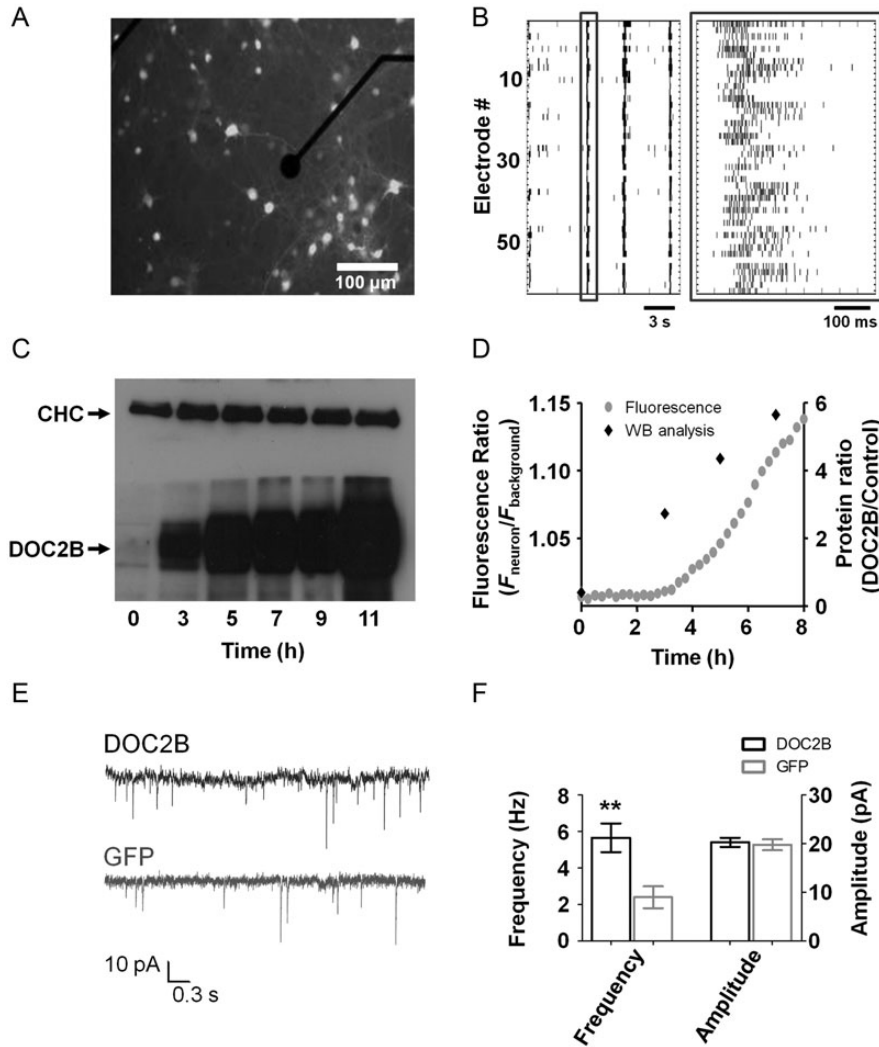
Figure 1. Cortical network on microelectrode array (MEA) overexpressing DOC2B. (*A*) Fluorescent cells overexpressing DOC2B and GFP on a MEA plate show high infection efficiency. The black circle is a 30-μm-diameter electrode embedded in the MEA plate (scale bar 100 μm). (*B*) Raster plot of spontaneous network activity recorded from the MEA plate consisting of periods of network-wide synchronized activity in the form of network bursts followed by periods of relative quiescence. Each black bar denotes a spike. Each row represents the activity recorded by a single electrode. One of the network bursts is enclosed in a dark gray square (right: zoom in on the single network burst demarcated with a dark gray square on the left) showing the high levels of activity in most electrodes at the beginning of the burst that ceases gradually. (*C*) Western blot (WB) analysis 3, 5, 7, 9, and 11 h after application of the DOC2B virus shows a gradual increase in DOC2B expression levels with no change in the level of the control protein (clathrin heavy chain, CHC). (*D*) Integrated analysis of GFP fluorescence and DOC2B protein levels as extracted by the WB analysis shows that DOC2B expression starts already 3–5 h after infection (right axis), concomitant with the increase in GFP fluorescence intensity over time (left axis). (*E*) Excitatory spontaneous activity (mEPSC) recorded in the presence of TTX and PTX from neurons in microislands overexpressing DOC2B (DOC2B, top trace) or the control green fluorescent protein (GFP, bottom trace). (*F*) DOC2B overexpression increased mEPSC frequency but did not change the amplitude of single mEPSCs (**$P < 0.01$, Student's *t*-test, 14 DOC2B and 12 GFP cultures).

course of GFP fluorescence increase following DOC2B-IRES-GFP infection using time-lapse imaging. Western blot analysis demonstrated that the expression level of DOC2B starts to increase 3 h after infection, reaching ~12-fold increase after 6 h (Fig. 1*C*,*D*; $n = 6$ cultures). Accordingly, GFP fluorescence began to increase as early as 3–4 h after infection and continued to increase linearly up to 8 h ($n = 4$ cultures, Fig. 1*D*). We thus performed all our measurements 5–7 h after infection with the Semliki Forest virus and visually confirmed GFP fluorescence in each recording. We assume that DOC2B is already localized in synapses at the time of experiments as previous work by Groffen et al. (2006) showed that 6–9 h after infection DOC2B was already localized in synapses. Immunofluorescence quantification of NeuN, a neuronal nuclei marker, in neuronal cultures infected with the DOC2B-

expressing virus showed infection was restricted mainly to neurons (Supplementary Fig. S1*A*, 86.5 ± 1.2% of the cells that were infected by the virus were neurons) and that ~50% of the neurons in the network were infected by the virus (50.8 ± 1.8%, $n = 12$ cultures). To rule out effects on the levels of other synaptic proteins, we used western blot to analyze the expression levels of key presynaptic and postsynaptic proteins and found that the levels of Munc18-1, Munc13-1, Synaptotagmin1, Tomosyn, NR2B, GluR2, Clathrin heavy chain, and PSD95 were not altered following DOC2B overexpression (Supplementary Fig. S1*C*).

To verify that DOC2B overexpression enhanced spontaneous release in our system, as previously described by Groffen et al. (2010), we recorded spontaneous neurotransmitter release by patching a single neuron in small neuronal

networks consisting of 20–100 cortical neurons grown on microislands (Lau and Bi 2005) in the presence of TTX and PTX. As expected we found a 2- to 3-fold increase in the frequency but not in the amplitude of excitatory mini release (mEPSC) following DOC2B overexpression (5.7 ± 0.8 Hz in 14 DOC2B-expressing microislands compared to 2.4 ± 0.6 Hz in 12 control GFP microislands; mean $\pm$ SEM; $P < 0.01$ Student's t-test; Fig. 1E,F).

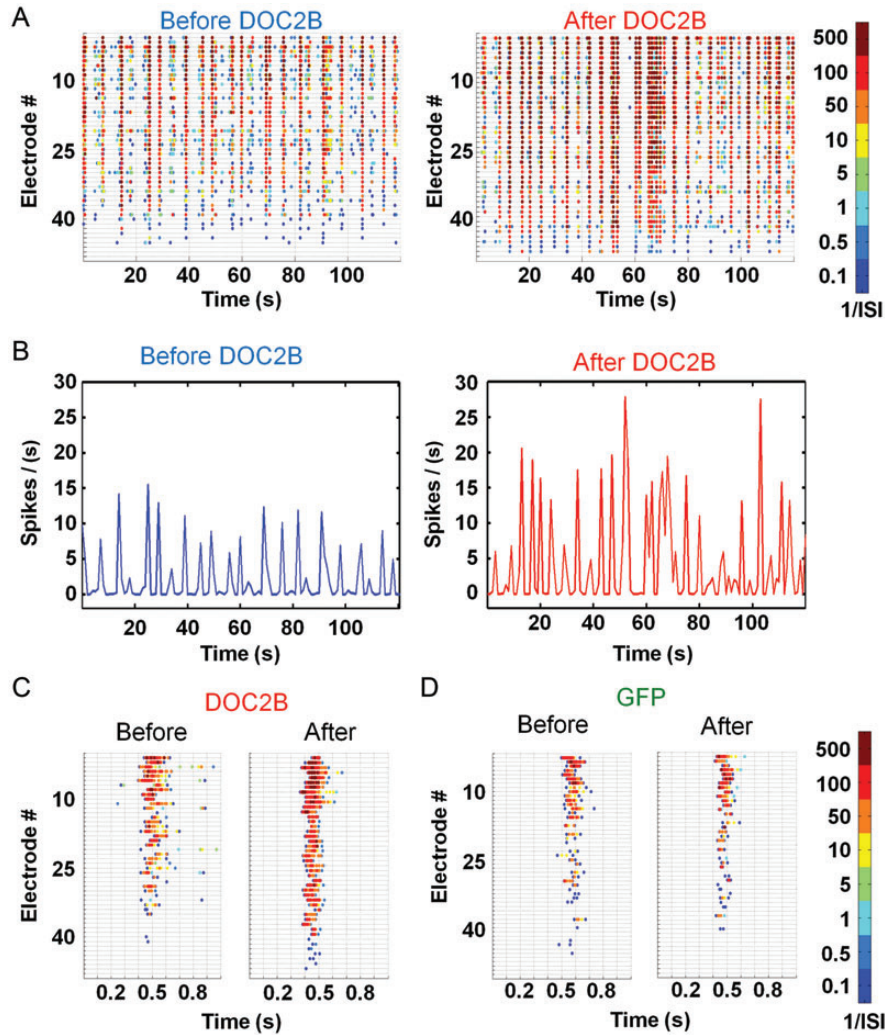### DOC2B Overexpression Increases Firing Rate Within Network Bursts

Understanding the effect of DOC2B overexpression on the activity of neuronal networks cultured on MEA plates was done by recording 1 h of spontaneous activity before DOC2B expression and 1 h of spontaneous activity 5–6 h after the introduction of the DOC2B-carrying virus. Hence, each experiment had its internal control in the form of activity before the application of the virus. Control recordings were done in a similar manner on neuronal networks expressing the GFP-carrying virus. For each recording, we generated color-coded raster plots, based on the average interspike interval for each spike in each electrode (Fig. 2A; 120 s of a sample recording before and after DOC2B overexpression). DOC2B overexpression increased the global spike rate ($49 \pm 10\%$, $P < 0.001$ Student's t-test; Fig. 3E) and the activity within network bursts, but did not change the frequency of network bursts (Fig. 2B; firing rate profile of the activity shown in Fig. 2A). Specific analysis of network bursts (Fig. 2C; single network bursts from each sample recording displayed at Fig. 2A) showed that DOC2B overexpression not only significantly increased the firing rate within the network burst (i.e., more spikes in each network burst; $24 \pm 6\%$, $P < 0.01$ Student's t-test; Fig. 3E), but it also significantly increased the number of electrodes participating in the network bursts (i.e., the number of electrodes recording neuronal activity in the network bursts was increased; $8 \pm 2\%$, $P < 0.01$ Student's t-test; Figs 2C and 3E). Surprisingly, DOC2B did not enhance the average number of spikes between network bursts ($10 \pm 33\%$) and did not change the interburst interval ($-12 \pm 11\%$). Notably, the control GFP virus did not induce any significant change in the burst activity parameters (Figs 2D and 3E, light-gray bars). We further examined the effect of DOC2B on the spiking pattern within network bursts by generating network-burst profiles (see Materials and Methods section and Eytan and Marom 2006). We aligned all network bursts in a single experiment to their time of initiation and averaged the firing rate throughout the network burst (Fig. 3A; sample recording before and after overexpression of DOC2B). In the specific example shown in Figure 3A, it is clearly seen that the network-burst profile reached higher values after DOC2B overexpression while the duration was not significantly altered ($4 \pm 3\%$). To quantify these effects, we averaged all DOC2B recordings before and after DOC2B overexpression (Fig. 3B). The network-burst profiles reached peak activity within approximately 100–150 ms from the beginning of the burst and then decayed slowly up to 1.5 s (Fig. 3B). Examination of the average network-burst profiles before and after introduction of DOC2B showed a 19% increase in the average firing rate that began around the burst's peak (Fig. 3B, full arrow) and lasted throughout the burst (Fig. 3B; for each recording, the firing rate was averaged by the number of

recording electrodes to avoid inter-recording bias, see Materials and Methods section for more details). In contrast, GFP overexpression caused a slight insignificant decrease in average burst firing rate.

Baseline MEA recordings showed high variability in spontaneous activity between different neuronal cultures. To overcome this variability and isolate the contribution of DOC2B to the spiking burst profile, we subtracted the burst profile before DOC2B of each recording from that after DOC2B overexpression and averaged over all DOC2B recordings. The same procedure was also performed for the GFP-expressing cultures. It is clear that DOC2B networks show an increase of up to 6.7 Hz per electrode in average firing rate (Fig. 3C, ΔDOC2B, black trace) throughout the network burst while GFP networks show almost no change (Fig. 3C, ΔGFP, light-gray trace). These data, together with the finding that DOC2B does not enhance spike activity between the network bursts suggest an activity-dependent contribution of DOC2B to the neuronal network activity.

The Regulation of Asynchronous but Not Spontaneous Release by DOC2B Enhances Activity Within Network Bursts

DOC2B has been shown to positively regulate nonsynchronous synaptic release by enhancing both spontaneous neurotransmitter synaptic release (Groffen et al. 2010; Pang et al. 2011) and asynchronous synaptic release (Yao et al. 2011). To understand which of these molecular features elicits the effect on neuronal network activity, we utilized a combination of pharmacological and genetic manipulation tools. To mimic the effect of enhanced asynchronous release, we applied Strontium, which is known to increase asynchronous synaptic release (Goda and Stevens 1994; Xu-Friedman and Regehr 1999) on *wt* cultures. To mimic the effect of enhanced spontaneous release, we overexpressed the constantly active DOC2B^{D218,220N}, a mutated form of DOC2B, which has been previously shown to increase mini release in a calcium-independent manner 3 times greater than DOC2B overexpression (Groffen et al. 2010). We performed the analysis described above and extracted the network-burst profiles to isolate the effect of DOC2B^{D218,220N} expression and Strontium application on the activity of neuronal networks. Our results demonstrated that application of Strontium not only significantly increased the global firing rate ($133 \pm 28\%$, $P < 0.01$ Student's t-test; Fig. 3E) but also increased the firing rate within network bursts (Fig. 3D dark gray) in a manner very similar to the effect of DOC2B but with higher intensity ($172 \pm 32\%$ increase in the number of spikes and $44 \pm 10\%$ increase in the number of electrodes which record neuronal activity in network bursts; $P < 0.01$ Student's t-test; Fig. 3D,E) and with an up to 35-Hz increase in firing rate within the network bursts. It should be noted that application of low concentrations of Strontium elicited smaller elevation in burst activity mimicking more accurately DOC2B effects (Supplementary Fig. S2), and the effect also showed linear correlation with Strontium concentration. In contrast to the Strontium effects, DOC2B^{D218,220N} expression substantially decreased the firing rate within network bursts and the participation of neurons in the network bursts ($-39 \pm 8\%$ decrease in the number of spikes and $-18 \pm 5\%$ in the number of electrodes which record neuronal activity in network bursts; $P < 0.05$ Student's
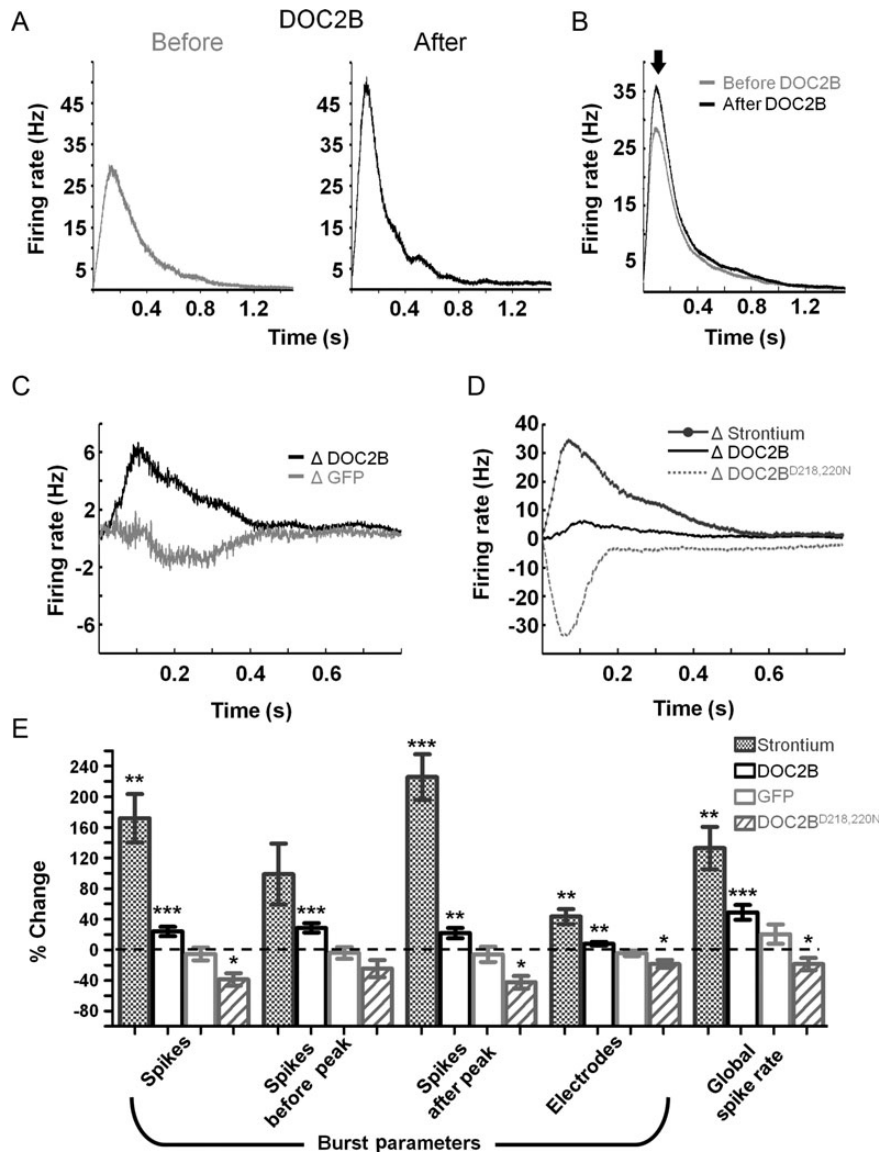
Figure 2. DOC2B overexpression increases average firing rate and the number of electrodes which participate in neuronal network bursts. (*A*) Color-coded raster plots displaying 2 min of spontaneous activity before (left) and after (right) overexpression of DOC2B. For every electrode (in each row), each spike is colored by the average interspike interval (1/ISI; electrodes are ordered by activity level, most active electrodes at the top). (*B*) Firing rate of spontaneous network activity shows an increase in the global firing rate (spike/s normalized by the number of active electrodes; taken from the same 2 min in *A*). (*C,D*) Color-coded raster plots focused to single networks burst emphasize the effect of DOC2B (*C*) and GFP (*D*) on network activity (taken from the same 2 min in *A*). (*C*) Following DOC2B overexpression, the spiking frequency in the network burst increases and more electrodes participate in it. (*D*) Following control GFP overexpression, the spiking frequency in the network and the number of participating electrodes do not change considerably.

t-test; Fig. 3*E*). These results suggest that enhancing asynchronous release increases firing rate during neuronal network bursts and that the enhancement of network-burst activity by DOC2B stems from its effect on asynchronous but not from spontaneous release. We therefore assumed that DOC2B overexpression and Strontium application would induce additional similar effects on the network activity that were uncovered in the following experiments.

To verify our assumption, we performed a more detailed analysis on the 2 postulated modes of activity of DOC2B. First, we analyzed the percentage of electrodes that participate in the network bursts. We created cumulative histogram representing the percentage of electrodes that were active in each burst. Evidently, following DOC2B overexpression and Strontium application, the ratio of electrodes which participate in network bursts increased, as indicated by the right-shifted curve (Fig. 4*A*). However, overexpression of DOC2B^{D218,220N} shifted the curve leftward and hence

decreased the participation of electrodes within network bursts. To better quantify these results, we used the method described by Eytan and Marom (2006) to identify full-blown and aborted network bursts. Bursts in which >50% of the electrodes participated were defined as full-blown bursts and bursts in which <50% of the electrodes participated were defined as aborted network bursts (Fig. 4*B*; full-blown bursts in black, aborted bursts in gray). DOC2B overexpression (Fig. 4*B*) and Strontium application significantly increased the ratio of full-blown bursts supporting the hypothesis that they induce a similar mode of action in the network level (Fig. 4*C*; *P* < 0.05 **P* < 0.01 Student's *t*-test). In contrast, DOC2B^{D218,220N} decreased this ratio compared with GFP control cultures. Higher ratio of full-blown bursts suggests that the same input that drives the network burst recruits more neurons for the network burst (Eytan and Marom 2006). This might come from enhanced synaptic transmission or from an increase in the activation of previously subthreshold nonactivated neurons (perhaps due to accumulation

Figure 3. Sustained DOC2B effect throughout the network burst. (*A*) A sample network-burst profile before (gray) and after (black) DOC2B overexpression shows the average firing rate throughout the network burst. DOC2B overexpression increases the average firing rate, specifically around the burst peak. (*B*) Average network-burst profiles from all DOC2B recordings before and after overexpression of DOC2B (gray and black traces, respectively; *n* = 15 DOC2B networks) show an increase in firing rate throughout the network burst. (*C*) To isolate the contribution of DOC2B to network activity for each experiment, the activity profile before DOC2B was subtracted from the activity profile after DOC2B and ΔDOC2B profile was generated (black trace) and averaged for all DOC2B experiments. The same procedure was applied to generate the ΔGFP profile (light-gray trace). As indicated by the black trace, following DOC2B overexpression, the average firing rate is higher throughout the burst while the ΔGFP profile displayed little change. (*D*) Average Δ network-burst profiles for Strontium application (dark-gray top trace; *n* = 6 Sr^{2+} networks) and DOC2B^{D218,220N} overexpression (light-gray bottom trace; *n* = 9 DOC2B^{D218,220N} network). Strontium application increases network-burst firing rate while DOC2B^{D218,220N} overexpression decreases network-burst firing rate. (*E*) Average change in global and burst parameters supports the profiles analysis in *D* and shows a significant increase in number of spikes and the number of neurons participating in network bursts for DOC2B overexpression and Strontium application and a significant decrease in the same parameters for DOC2B^{D218,220N} overexpression (comparison of each recording to itself prior to manipulation; 15 DOC2B recordings, 9 GFP recordings; 6 Strontium recordings, 9 DOC2B^{D218,220N} recordings; *$P < 0.05$, **$P < 0.01$, ***$P < 0.001$, Student's *t*-test).

of activity induced by the enhanced asynchronous release). In any case, it would suggest that the same synaptic output produced by the driving force of the network bursts now activates more neurons within the burst and the output/input ratio within the network burst increases (Eytan and Marom 2006; Eckmann et al. 2008).

Next, we analyzed the network synchronization in the different experimental conditions. Synchronization is a fundamental feature of neuronal network activity, allowing it to generate various activity rhythms and transmit information (Cobb et al. 1995; Wang and Buzsaki 1996). We further

investigated the interaction of spiking activity of neurons within the network burst by analyzing the network synchronization with the average pairwise Pearson correlation (Fig. 5*A*; as described in the Materials and Methods section). The synchronization was normalized by the number of participating electrodes and the firing rate of each burst to isolate the synchronization pattern. To account for interculture variability, we subtracted the synchronization before manipulation from the synchronization after manipulation and averaged over all recordings. Cultures overexpressing DOC2B and cultures with Strontium displayed a significant increase in synchronization,
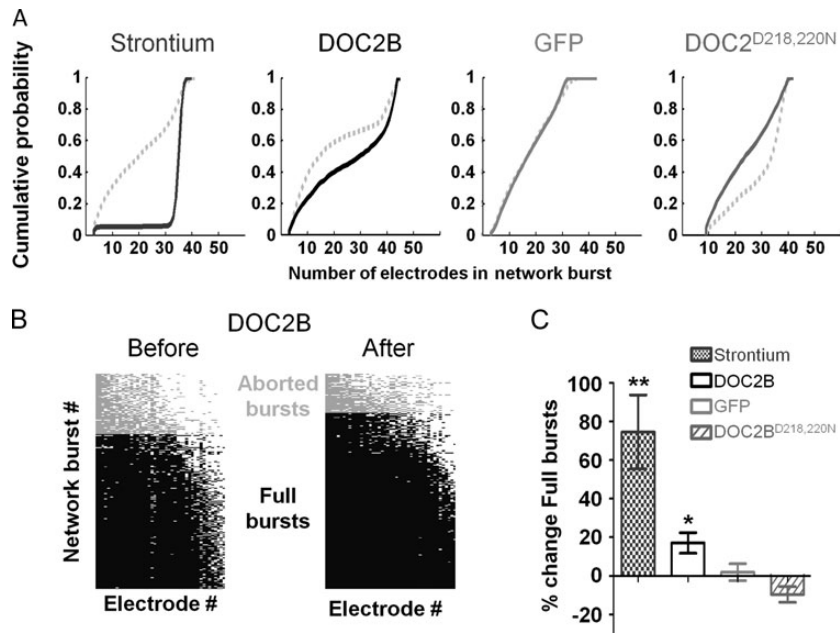
Figure 4. Participation of electrodes in network bursts is elevated following DOC2B overexpression and Strontium application. (*A*) Cumulative probability of electrode participation in network burst for Strontium application, DOC2B, GFP, and DOC2B^{D218,220N} overexpression (from left to right, respectively). While DOC2B overexpression and Strontium application right shifted the cumulative probability of neuron participation in network bursts, DOC2B^{D218,220N} overexpression shifted the cumulative probability leftward (control: broken gray line). (*B*) Participation of electrodes in network burst before (left) and after (right) overexpression of DOC2B. The electrodes participating in each network burst, sorted by activity level, show a significant increase following DOC2B overexpression (each column marks the participation of a single electrode across all network bursts; each row marks the electrodes participating in a single network burst; network bursts with the highest number of active electrodes on the bottom; electrodes that participated in all of the network bursts on the left; light-gray bars indicate aborted network bursts (on the top) and black bars indicate full-blown network bursts (on the bottom). (*C*) Following DOC2B overexpression and Strontium application, the ratio of full network bursts is significantly increased (*$P < 0.05$, **$P < 0.01$, Student's *t*-test), while GFP networks show no change and DOC2B^{D218,220N} networks show a decrease in the ration of full-blown bursts.

primarily around the burst's peak. However, cultures expressing DOC2B^{D218,220N} exhibited a reduction in average synchronization (Fig. 5*B*).

Taken together, the results above suggest that the effect of DOC2B overexpression on neuronal network activity is similar in several aspects to the effect elicited by Strontium application. As the increase in Strontium concentration is linearly correlated with the increase in peak network-burst firing rate (Supplementary Fig. S2), we suggest for the first time that, by promoting asynchronous release in the neuronal level, DOC2B increases the synchronization on the network level. To understand how an increase in asynchronous release in the neuronal level could account for increased activity during network bursts, we utilized a computational model.

Our model was based on a postsynaptic neuron, which receives inputs from 10 presynaptic neurons (presynaptic events) and integrates them to changes in its membrane potential (EPSPs; Fig. 6*A*; leaky integrate-and-fire neuron). If the membrane potential passed a specific threshold (Fig. 6*B*; dashed line), the neuron fired an action potential and the number and frequency of action potentials were measured as the output of this neuron. The model simulated the response of the neuron to presynaptic inputs at low-frequency between bursts (0.5 Hz; baseline condition from 10 presynaptic neurons) and high-frequency within bursts (1–5 Hz). We simulated the increased asynchronous release as additional presynaptic events with lower amplitude that decayed exponentially (see Materials and Methods section) and tested the number of action potentials elicited by the postsynaptic neuron under various frequencies of presynaptic events

(Fig. 6*B*; various burst intensities). It was clear that increased asynchronous release rendered the neuron more sensitive to presynaptic events, and thus it became more active at lower input frequencies (Fig. 6*B*). Consequently, the same input spike frequency caused the neuron to generate more action potentials as the contribution of the asynchronous release increased. Interestingly, a 10-fold increase in asynchronous release, which markedly increased the action potential elicited within bursts, did not cause the neuron to generate action potentials at baseline condition (i.e., between bursts; Fig. 6*C*; 0.5-Hz simulated baseline condition between bursts). This model could explain how an increase in asynchronous release by DOC2B and Strontium can increase the network-burst activity within the bursts without increasing the firing rate and the number of spikes between network bursts.

Munc13-1 Overexpression Decreases Network Burst Firing Rate but Increases Network-Burst Frequency
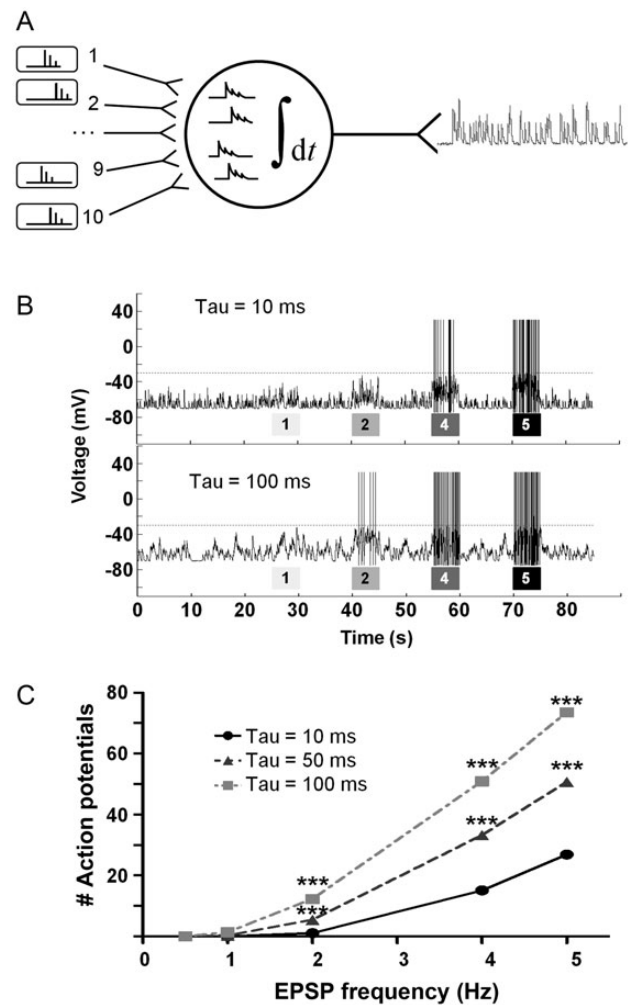
Both DOC2B and Munc13-1 are known as proteins that promote synaptic transmission, albeit in different mechanisms. While DOC2B enhances spontaneous and asynchronous release (nonsynchronous), Munc13-1 is known to enhance vesicle maturation and priming of synaptic vesicles in general (Betz et al. 1998; Augustin et al. 1999; Tokumaru and Augustine 1999; Ashery et al. 2000; Lou et al. 2005, 2008; Weimer et al. 2006). We utilized the Semliki Forest virus to express Munc13-1-GFP in neuronal cultures plated on MEAs and compared its effect on network activity to cultures infected with GFP virus (recording was performed in the same manner as
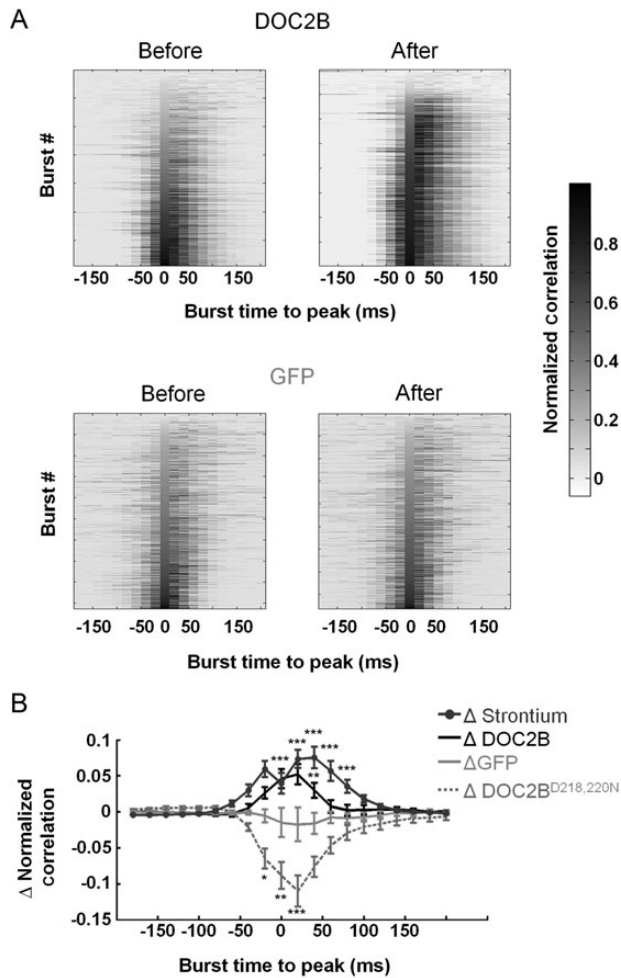
Figure 5. DOC2B and Strontium enhance network burst synchronization. (*A*) Average pairwise Pearson correlation (synchronization) before and after DOC2B (top) and GFP (bottom) overexpression. Each row represents the correlation ±200 ms around the peak (20 ms bin, peak at 0) of each network burst (correlation is normalized by the peak firing rate of each burst). Bursts are aligned to their peak and ordered by correlation at the peak of the burst. Clearly, DOC2B overexpression increases the network-burst synchronization, primarily around the peak as indicated by darker shades (Color bar indicates the average normalized Pearson correlation for each bin). (*B*) Average change in normalized pairwise Pearson correlation demonstrates the significant contribution of DOC2B and Strontium to network synchronization (*$P < 0.05$, **$P < 0.01$, ***$P < 0.001$, ANOVA for repeated measurements).

Figure 6. Increased asynchronous release enhances a model-neuron response to presynaptic input. (*A*) The membrane potential of a postsynaptic leaky integrate-and-fire neuron was simulated as it integrated presynaptic events to EPSPs (baseline frequency 0.5 Hz) from 10 presynaptic neurons at various frequencies. The parameters of the EPSPs (amplitude and decay kinetics) were measured experimentally from cultured neurons and were used as a baseline parameter for EPSP kinetics (baseline EPSP decay time constant of 52 ms; EPSP amplitude 7 mV). (*B*) The model simulated periods of low input frequency (representing periods between bursts) and periods of intense input frequency (representing periods of bursts) under 3 different asynchronous release conditions (i.e., 3 different decay time constants). Asynchronous release was simulated by changing the presynaptic input synchrony which decayed with an exponential decay coefficient ranging from 10 to 100 ms (Tau). For each asynchronous release condition, the Tau remained constant while the EPSP spike frequency was changed between 1, 2, 4, and 5 Hz (indicated by the gray bars under the voltage trace) for 5 s and then changed back to baseline frequency. Gray dashed line indicated voltage threshold for action potential. More action potentials were elicited under EPSPs with longer time constants (bottom trace). (*C*) Higher asynchronous release decay coefficient increased the number of action potentials generated by the neuron during periods when input frequency was >1 Hz (i.e., periods of bursts; on average per presynaptic neuron; in comparison to baseline decay coefficient; ***$P < 0.001$, ANOVA for repeated measurements).

described above for DOC2B). As with DOC2B, we verified the expression efficiency and found that 37% of the neurons were overexpressing Munc13-1 along with a 2-fold increase in the expression level of Munc13-1. Examination of the spontaneous network activity recorded before and after Munc13-1 overexpression produced several findings: first, an increase in the total number of spikes per minute as predicted from a protein that enhances synaptic release ($18 \pm 6\%$, $P < 0.05$ Student's *t*-test). In addition, we discovered 2 interesting changes in the pattern of the network bursts: a significant decrease in firing rate within network bursts ($-29 \pm 6\%$ $P < 0.01$ Student's *t*-test; Fig. 7*A*,*C*) and an increase in the frequency of network bursts indicated by a $42 \pm 6\%$ decrease in the interburst interval ($P < 0.01$ Student's *t*-test; Fig. 7*B*). We further analyzed the network-burst profiles to isolate the effect of Munc13-1 (Fig. 7*C*; as described above by subtracting the activity of each recording from itself prior to manipulation), and found

that throughout the network burst, Munc13-1 decreased the firing rate by 9 Hz (Fig. 7*D*). Thus, it appears that although both DOC2B and Munc13-1 positively regulate synaptic transmission and enhance the number of spikes in the network, Munc13-1 has an opposite effect to the effect of DOC2B on the activity within the burst. A possible explanation for this is the ability of Munc13-1 to enhance priming for synchronous and nonsynchronous synaptic release (Augustin et al. 1999;
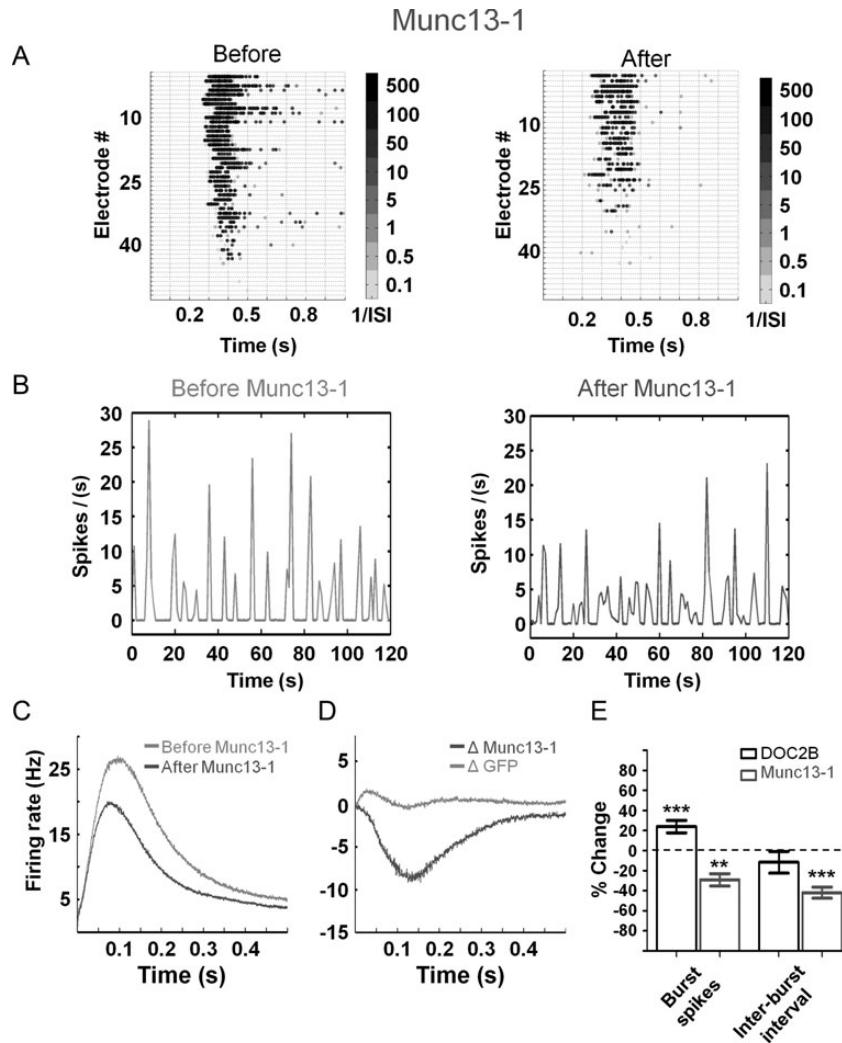
Figure 7. Munc13-1 redistributes network spiking activity. (*A*) Gray-scale raster plots demonstrate that Munc13-1 overexpression decreases the spiking frequency in the network bursts (indicated by the brighter colors). (*B*) Network firing rate (normalized per electrode) before and after Munc13-1 overexpression (sample recording; representative trace). While each network burst shows lower spiking activity, the prevalence of network bursts is increased following Munc13-1 overexpression. (*C*) Average network-burst profiles from all recordings before (light-gray) and after (dark-gray) overexpression of Munc13-1 (*n* = 11 Munc13-1 networks). (*D*) The change in the network-bursts spiking profile following Munc13-1 overexpression. Munc13-1 overexpression decreases network-burst firing rate by 9 Hz while GFP overexpression induces almost no change. (*E*) Comparison of DOC2B and Munc13-1 overexpression effects on network activity parameters. While Munc13-1 overexpression decreases the number of spikes within network bursts by 29%, it increases the frequency of network-burst occurrence by 42% (as evident in the decreased interburst interval; **$P < 0.01$ ***$P < 0.001$ Student's *t*-test).

Tokumaru and Augustine 1999; Ashery et al. 2000; Lou et al. 2005, 2008; Weimer et al. 2006). It is possible that by increasing the readiness of vesicles for release in each neuron, Munc13-1 enhances the occurrence of bursting activity on the network level, even before full replenishment of vesicles occurs in each neuron. This in turn leads to recurring bursting activity in which each burst displays a lower level of activity (both in the number of spikes and the peak firing rate).

Comparing the network effects of DOC2B and Munc13-1 overexpression reveals the connection between their effect on the single-neuron level and the network level. While DOC2B increases the number of spikes in network bursts, it does not change the frequency of network-burst occurrence; however, Munc13-1 clearly decreases the number of spikes in network bursts while increasing the frequency of network-burst occurrence (Fig. 7*E*; increased burst occurrence is indicated by the reduced interburst interval; **$P < 0.01$ ***$P < 0.001$, Student's *t*-test). Thus, although DOC2B and Munc13-1 enhance vesicle

fusion to facilitate synaptic release in the cellular level (Betz et al. 1998; Friedrich et al. 2008), they seem to display different effects on the network level.

Discussion

Utilizing the unique advantages of the MEA system, we examined how DOC2B and Munc13-1 contribute to neuronal network activity. Although DOC2B and Munc13-1 share the ability to enhance vesicle fusion and facilitate synaptic release in the cellular level, we show here for the first time that they display different effects on the network level. While the firing rate within network bursts was increased by DOC2B, it was reduced by Munc13-1; however, Munc13-1 increased the rate of network bursts. This difference emphasizes that enhancement of synaptic release is an intricate process that might have different manifestations in the single-neuron level and in the network level.

DOC2B Enhances Activity Within Network Bursts by Increasing Asynchronous Release

DOC2B has been previously implicated as a positive promoter of activity-dependent exocytosis (Groffen et al. 2006; Friedrich et al. 2008) which enhances spontaneous and asynchronous neurotransmitter release (Groffen et al. 2010; Pang et al. 2011; Yao et al. 2011). Here, we demonstrated for the first time its effects on neuronal network activity, which suggest that DOC2B has a functional role in the regulation of bursting activities in neuronal networks. Using the unique advantages of the MEA system (Stegenga et al. 2008; Chiappalone et al. 2009), we were able to record the activity of cortical neurons before and after expression of DOC2B, overcome the interculture variability and isolate the contribution of DOC2B to the neuronal network activity profile. This contribution was reflected in an augmentation of the number of spikes and an increase in the number of active neurons during the network burst. Although DOC2B was previously shown to increase asynchronous and spontaneous synaptic release, DOC2B overexpression did not cause a homogeneous increase in neuronal network activity, as one might have predicted, but rather caused a specific increase in neuronal activity only during network bursts.

To understand the contribution of DOC2B to network activity, we applied a combination of pharmacological tools, genetic manipulations, and computational simulation. As significant knockdown of DOC2B takes several days to reach full potential (Pang et al. 2011; Yao et al. 2011) and we wanted to avoid adaptation processes that can occur during this period, we focused our experiments on enhancing the molecular properties of DOC2B by overexpression. As Strontium application enhances asynchronous release (Goda and Stevens 1994; Xu-Friedman and Regehr 1999; Shin et al. 2003), we utilized Strontium to mimic the effect of DOC2B in promoting asynchronous release (Yao et al. 2011). Indeed, application of Strontium acted in the same manner as DOC2B overexpression by increasing the network-burst activity, the ratio of full-blown bursts and the network-burst synchronization. Next, we utilized the mutated form of DOC2B, DOC2B^{D218,220N}, which has been shown to constantly increase the rate of spontaneous release in a calcium-independent manner up to 3 times more than DOC2B (Groffen et al. 2010). The effect of this mutant on the network level was a decrease in the firing rate and in the synchronization within network bursts. It should be noted that although the contribution of DOC2B^{D218,220N} to asynchronous release has not been shown, it is unlikely that overexpression of DOC2B^{D218,220N} would lead to an increase in asynchronous release but rather an overall increase in spontaneous release that causes synaptic depletion. This can be supported from experiments performed in DOC2B^{D218,220N}-expressing chromaffin cells showing a reduced sustained release component and depression during repeated stimulation (Friedrich et al. 2008). Therefore, we suggest that it is the role of DOC2B in enhancing the asynchronous release, but not the spontaneous release, that enhances network bursts. Furthermore, assuming that spontaneous, asynchronous, and synchronous release share the same resources for synaptic release (as suggested by Pang et al. 2006; Sun et al. 2007 but see Sara et al. 2005; Fredj and Burrone 2009), it is clear why superfluous spontaneous release in DOC2B^{D218,220N} suppresses synchronous and asynchronous release. Cohen and Segal (2011)

showed that lower availability of releasable vesicles reduced the activity within network bursts. Assuming a zero-sum hypothesis for the number of available vesicles, one can assume that a massive increase in the spontaneous activity seen in DOC2B^{D218,220N} (Groffen et al. 2010) would decrease the size of the releasable vesicle pools, leading to reduced vesicle availability and reduced release during the bursts. Nevertheless, as this mutated form of DOC2B might cause other changes in the synapse, other possibilities should be considered.

The connection between an increase in asynchronous release in the single-neuron level and increased network-burst activity has been described in the past (Lau and Bi 2005; Jones et al. 2007). To understand how this increase in firing rate occurs exclusively within bursts upon an increase in asynchronous release by both DOC2B and Strontium, we simulated the response of a neuron to presynaptic inputs within bursts and between bursts. Our model predicted that an increase in the asynchronous phase of the EPSP allows better temporal and spatial summation and increases the response on the neuron only for higher presynaptic input frequencies (>1 Hz for the parameter used in the model). Under these conditions, the probability for summation increases and synaptic integration increases the frequency of action potentials only within bursts. This explains how an increase in asynchronous release could lead to an increase in network-burst spiking activity without increasing interburst activity. As the increase of asynchronous release by DOC2B and Strontium induced changes in the network activity, DOC2B might carry a functional role in tuning network-bursting activity in the behaving animal.

Munc13-1 and DOC2B: Interacting Partners in the Molecular Level Display Opposite Effects in the Network Level

As for DOC2B, Munc13-1 has been shown to promote synaptic release (Betz et al. 1998; Ashery et al. 2000; Basu et al. 2007). To understand if this property causes the same effect on network activity, we examined the effects of Munc13-1 on neuronal activity. Surprisingly, Munc13-1 decreased the firing rate within network bursts but increased the frequency of network bursts. This means that, in general, Munc13-1 increased the bursting rhythm of the network but each burst transmitted less spikes. As the termination of bursts might occur upon depletion of presynaptic vesicles (Cohen and Segal 2011), it is reasonable to assume that smaller bursts following Munc13-1 overexpression come from an insufficient refilling process (providing fewer resources for the next network burst). As Munc13-1 overexpression caused short-term synaptic depression upon repeated stimulation (Rosenmund et al. 2002), it is possible that Munc13-1 overexpression destabilizes the balance between the priming and the replenishment processes. However, as Munc13-1 enhances vesicle priming, it increases the readiness of vesicles for release in single neurons (Ashery et al. 2000; Rettig and Neher 2002; Martin 2003; Rosenmund et al. 2003), and this enhances the occurrence of bursting activity on the network level, even before the full replenishment of vesicles occurs in each neuron. Yet, further studies are required to understand the exact link between the effects on the cellular level and the effects on network activity of Munc13-1. Furthermore, as DOC2B and Munc13-1 interact in the cellular level through the DOC2 Munc13-interacting domain (Mochida et al. 1998;

Duncan et al. 1999) further and more detailed analysis should be made to dissect the contribution of this interaction to the changes in the network-bursting activity.

Although key synaptic proteins affect a clear physiological activity at the neuronal level, the network activity is driven by the complex interaction between neurons, which might filter out or amplify various functional properties (McKinney et al. 1999; Otsu and Murphy 2003). As illustrated in Figure 8A, since DOC2B increases asynchronous release on the neuronal level its effect on network level focuses primarily on network bursts. However, Munc13-1, which enhances vesicle priming, induces redistribution of spiking activity in the network level (Fig. 8B) reducing activity within the bursts but increasing burst frequency. Thus, although DOC2B and Munc13-1 share the ability to enhance vesicle fusion to facilitate synaptic release in the cellular level (Betz et al. 1998; Yao et al. 2011), they display different effects on the network level. This difference emphasizes that enhancement of synaptic release is an intricate process that might have different manifestations in the single-neuron level and in the network level. The novel platform presented in this work also highlights the complementary role of the network level in explaining the physiological relevance of presynaptic proteins.

Physiological Relevance

The above results suggest that the expression level and activity of presynaptic proteins can control network-wide
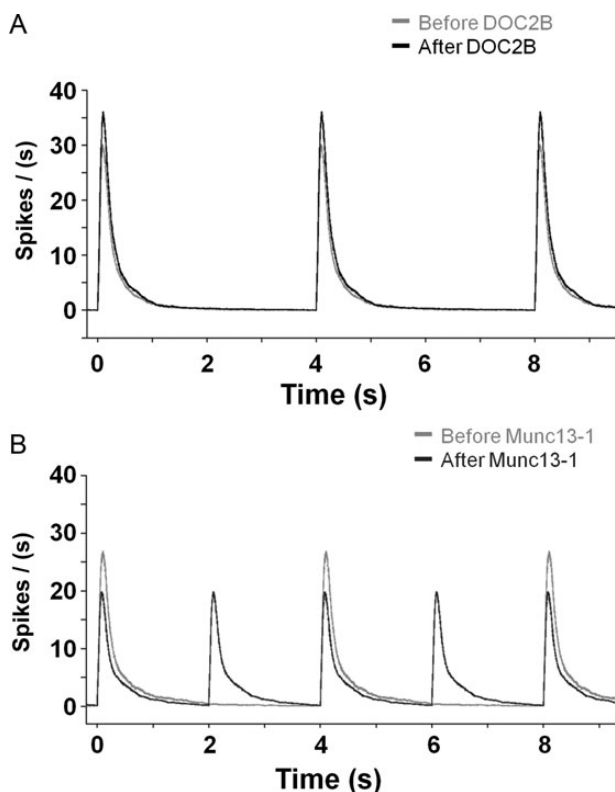
Figure 8. Illustration of DOC2B and Munc13-1 impact on network-bursting activity shows divergent effects. While DOC2B enhances the activity within network bursts, it does not change the occurrence of network bursts (A; DOC2B-black, control-gray). However, Munc13-1 decreases the network spiking activity within the burst but enhances bursts frequency (B; Munc13-1: dark gray, control: light-gray). The network-burst profiles are based on the average firing rates in Figures 3 and 7.

activity. It is especially interesting to note that the effect of Munc13-1 on the bursting pattern of the neuronal network was achieved by its expression in 37% of the neurons with only a 2-fold increase in protein quantity. Such changes in the expression levels are physiologically plausible (Guzowski et al. 2001; Ronnback et al. 2005; Toscano et al. 2006). Furthermore, plasticity-dependent changes in the activity of synaptic proteins can occur on the seconds time scale and lead to immediate changes in network activity (Huang and Kandel 1994; Malenka and Nicoll 1999; Castillo et al. 2002; Rosenmund et al. 2002); Proteins like Munc13-1 and DOC2B can be activated by calcium, Calmodulin, and diacylglycerols, which can boost their activity without the need for translational modifications. Hence, changes in protein expression or their activity levels can act as a wider mechanism to tune the bursting regime of neuronal networks.

What could be the implications of these changes on the function and activity of neuronal networks in the neocortex? A growing body of evidence connects between the recurrent synchronized activity in the form of network bursts displayed by dissociated cortical cultures in vitro and the rhythmic transition between up and down states identified in the neocortex in vivo (Baltz et al. 2010; Gullo et al. 2010, 2012; Becchetti et al. 2012; Hinard et al. 2012). These complex neocortical rhythmic activities have been linked to sensorimotor gating, short-term memory storage, and selective attention (Goldman-Rakic 1995; Luck et al. 1997; Sanchez-Vives and McCormick 2000; Timofeev et al. 2000, 2001; Shu et al. 2003). It has been even suggested that cultured neuronal network present sleep-like activity (Hinard et al. 2012) by displaying recurrent bursting periods followed by silent periods reminiscent of the activity of cortical neuron in vivo during sleep (Steriade et al. 1993; Timofeev et al. 2000). Interestingly, the oscillatory nature of up and down states could be explained by a modulation of presynaptic release. Specifically, it has been suggested that while nonsynchronous synaptic release might maintain the up-state (Timofeev et al. 2000, 2001), synaptic depression could be used to terminate it and return the activity to the down state (Hill and Tononi 2005).

As DOC2B and Munc13-1 change the pattern of bursting and synchronization of neuronal networks, they could modulate the patterns of up and down states. DOC2B, by increasing asynchronous release, could increase the synchronization of the network in the up-state and, as suggested by our computational model, could facilitate the sensitivity of the network to external input. Alternatively, as Munc13-1 changes the frequency of bursts, it could change the rate of transitions between up and down and increase short-term memory capacity and storage (McCormick 2005; Holcman and Tsodyks 2006; Miller and Wang 2006). In general, activation or attenuation of specific synaptic proteins might serve as a powerful computational tool to tune the information flow and regulate higher functions in the neocortex in vivo (Silva et al. 1996; Dyck et al. 2009, 2011; Blundell et al. 2010; Chen et al. 2011). Interestingly, lack of synchronous release but enhanced asynchronous release following Synaptotagmin-1 KO in the hippocampal CA1 region did not impede acquisition of contextual fear memories; however, it did impair their precision. This suggests that the hippocampal CA1 region can rely on spike bursts to transfer information downstream (Xu et al. 2012). Therefore, modulation of bursting activity accompanying short- or long-term plasticity can control information

transfer for complex behaviors in the level of the animal. Nevertheless, the link between neuronal firing, information content, and physiological relevance is only emerging, and further experiments and analyses are needed.

Simultaneous measurement of activity from a large number of neurons has become a key method in the efforts to understand neuronal coding (Brown et al. 2004; Buzsaki 2004; Stevenson et al. 2008; Weihberger et al. 2012). As synaptic proteins are determinant elements in the activity of synapses, they play a crucial role in shaping the activity of neuronal networks (Chiappalone et al. 2009). This, in turn, is linked almost directly to the plasticity and computational abilities of the network. This study presented an innovative platform to investigate the functional role of synaptic manipulations in the network level. An integrated understanding of synaptic protein physiology at the cellular and network levels promises to uncover the organizing principles of neuronal network activity.

Supplementary Material

Supplementary material can be found at: http://www.cercor. oxfordjournals.org/.

References

Ashery U, Betz A, Xu T, Brose N, Rettig J. 1999. An efficient method for infection of adrenal chromaffin cells using the Semliki Forest virus gene expression system. Eur J Cell Biol. 78:525–532.

Ashery U, Varoqueaux F, Voets T, Betz A, Thakur P, Koch H, Neher E, Brose N, Rettig J. 2000. Munc13-1 acts as a priming factor for large dense-core vesicles in bovine chromaffin cells. EMBO J. 19:3586–3596.

Augustin I, Rosenmund C, Sudhof TC, Brose N. 1999. Munc13-1 is essential for fusion competence of glutamatergic synaptic vesicles. Nature. 400:457–461.

Baltz T, de Lima AD, Voigt T. 2010. Contribution of GABAergic interneurons to the development of spontaneous activity patterns in cultured neocortical networks. Front Cell Neurosci. 4:15.

Baruchi I, Ben-Jacob E. 2007. Towards neuro-memory-chip: imprinting multiple memories in cultured neural networks. Phys Rev. 75:050901.

Basu J, Betz A, Brose N, Rosenmund C. 2007. Munc13-1 C1 domain activation lowers the energy barrier for synaptic vesicle fusion. J Neurosci. 27:1200–1210.

Becchetti A, Gullo F, Bruno G, Dossi E, Lecchi M, Wanke E. 2012. Exact distinction of excitatory and inhibitory neurons in neural networks: a study with GFP-GAD67 neurons optically and electrophysiologically recognized on multielectrode arrays. Front Neural Circuits. 6:63.

Betz A, Ashery U, Rickmann M, Augustin I, Neher E, Sudhof TC, Rettig J, Brose N. 1998. Munc13-1 is a presynaptic phorbol ester receptor that enhances neurotransmitter release. Neuron. 21:123–136.

Betz A, Thakur P, Junge HJ, Ashery U, Rhee JS, Scheuss V, Rosenmund C, Rettig J, Brose N. 2001. Functional interaction of the active zone proteins Munc13-1 and RIM1 in synaptic vesicle priming. Neuron. 30:183–196.

Blundell J, Kaeser PS, Sudhof TC, Powell CM. 2010. RIM1alpha and interacting proteins involved in presynaptic plasticity mediate prepulse inhibition and additional behaviors linked to schizophrenia. J Neurosci. 30:5326–5333.

Brown TH, Kairiss EW, Keenan CL. 1990. Hebbian synapses: biophysical mechanisms and algorithms. Annu Rev Neurosci. 13:475–511.

Brown EN, Kass RE, Mitra PP. 2004. Multiple neural spike train data analysis: state-of-the-art and future challenges. Nat Neurosci. 7:456–461.

Buzsaki G. 2004. Large-scale recording of neuronal ensembles. Nat Neurosci. 7:446–451.

Castillo PE, Schoch S, Schmitz F, Sudhof TC, Malenka RC. 2002. RIM1alpha is required for presynaptic long-term potentiation. Nature. 415:327–330.

Chen K, Richlitzki A, Featherstone DE, Schwarzel M, Richmond JE. 2011. Tomosyn-dependent regulation of synaptic transmission is required for a late phase of associative odor memory. Proc Natl Acad Sci USA. 108:18482–18487.

Chiappalone M, Casagrande S, Tedesco M, Valtorta F, Baldelli P, Martinoia S, Benfenati F. 2009. Opposite changes in glutamatergic and GABAergic transmission underlie the diffuse hyperexcitability of synapsin I-deficient cortical networks. Cereb Cortex. 19:1422–1439.

Cobb SR, Buhl EH, Halasy K, Paulsen O, Somogyi P. 1995. Synchronization of neuronal activity in hippocampus by individual GABAergic interneurons. Nature. 378:75–78.

Cohen D, Segal M. 2011. Network bursts in hippocampal microcultures are terminated by exhaustion of vesicle pools. J Neurophysiol. 106:2314–2321.

Dimova K, Kalkhof S, Pottratz I, Ihling C, Rodriguez-Castaneda F, Liepold T, Griesinger C, Brose N, Sinz A, Jahn O. 2009. Structural insights into the calmodulin-Munc13 interaction obtained by cross-linking and mass spectrometry. Biochemistry. 48:5908–5921.

Duncan RR, Betz A, Shipston MJ, Brose N, Chow RH. 1999. Transient, phorbol ester-induced DOC2-Munc13 interactions in vivo. J Biol Chem. 274:27347–27350.

Dyck BA, Beyaert MG, Ferro MA, Mishra RK. 2011. Medial prefrontal cortical synapsin II knock-down induces behavioral abnormalities in the rat: examining synapsin II in the pathophysiology of schizophrenia. Schizophr Res. 130:250–259.

Dyck BA, Skoblenick KJ, Castellano JM, Ki K, Thomas N, Mishra RK. 2009. Behavioral abnormalities in synapsin II knockout mice implicate a causal factor in schizophrenia. Synapse. 63:662–672.

Eckmann JP, Jacobi S, Marom S, Moses E, Zbinden C. 2008. Leader neurons in population bursts of 2D living neural networks. New J Phys. 10:015011.

Eytan D, Marom S. 2006. Dynamics and effective topology underlying synchronization in networks of cortical neurons. J Neurosci. 26:8465–8476.

Fredj NB, Burrone J. 2009. A resting pool of vesicles is responsible for spontaneous vesicle fusion at the synapse. Nat Neurosci. 12:751–758.

Friedrich R, Groffen AJ, Connell E, van Weering JR, Gutman O, Henis YI, Davletov B, Ashery U. 2008. DOC2B acts as a calcium switch and enhances vesicle fusion. J Neurosci. 28:6794–6806.

Goda Y, Stevens CF. 1994. Two components of transmitter release at a central synapse. Proc Natl Acad Sci USA. 91:12942–12946.

Goldman-Rakic PS. 1995. Cellular basis of working memory. Neuron. 14:477–485.

Grillner S, Markram H, De Schutter E, Silberberg G, LeBeau FE. 2005. Microcircuits in action—from CPGs to neocortex. Trends Neurosci. 28:525–533.

Groffen AJ, Friedrich R, Brian EC, Ashery U, Verhage M. 2006. DOC2A and DOC2B are sensors for neuronal activity with unique calcium-dependent and kinetic properties. J Neurochem. 97:818–833.

Groffen AJ, Martens S, Diez Arazola R, Cornelisse LN, Lozovaya N, de Jong AP, Goriounova NA, Habets RL, Takai Y, Borst JG et al. 2010. Doc2b is a high-affinity Ca2+ sensor for spontaneous neurotransmitter release. Science. 327:1614–1618.

Gullo F, Maffezzoli A, Dossi E, Lecchi M, Wanke E. 2012. Classifying heterogeneity of spontaneous up-states: a method for revealing variations in firing probability, engaged neurons and Fano factor. J Neurosci Methods. 203:407–417.

Gullo F, Mazzetti S, Maffezzoli A, Dossi E, Lecchi M, Amadeo A, Krajewski J, Wanke E. 2010. Orchestration of "presto" and "largo" synchrony in up-down activity of cortical networks. Front Neural Circuits. 4:11.

Guzowski JF, Setlow B, Wagner EK, McGaugh JL. 2001. Experience-dependent gene expression in the rat hippocampus after spatial learning: a comparison of the immediate-early genes Arc, c-fos, and zif268. J Neurosci. 21:5089–5098.

Hausser M, Raman IM, Otis T, Smith SL, Nelson A, du Lac S, Loewenstein Y, Mahon S, Pennartz C, Cohen I et al. 2004. The beat goes on: spontaneous firing in mammalian neuronal microcircuits. J Neurosci. 24:9215–9219.

Hill S, Tononi G. 2005. Modeling sleep and wakefulness in the thalamocortical system. J Neurophysiol. 93:1671–1698.

Hinard V, Mikhail C, Pradervand S, Curie T, Houtkooper RH, Auwerx J, Franken P, Tafti M. 2012. Key electrophysiological, molecular, and metabolic signatures of sleep and wakefulness revealed in primary cortical cultures. J Neurosci. 32:12506–12517.

Holcman D, Tsodyks M. 2006. The emergence of Up and Down states in cortical networks. PLoS Comput Biol. 2:e23.

Huang YY, Kandel ER. 1994. Recruitment of long-lasting and protein kinase A-dependent long-term potentiation in the CA1 region of hippocampus requires repeated tetanization. Learn Mem. 1:74–82.

Jones J, Stubblefield EA, Benke TA, Staley KJ. 2007. Desynchronization of glutamate release prolongs synchronous CA3 network activity. J Neurophysiol. 97:3812–3818.

Junge HJ, Rhee JS, Jahn O, Varoqueaux F, Spiess J, Waxham MN, Rosenmund C, Brose N. 2004. Calmodulin and Munc13 form a Ca2+ sensor/effector complex that controls short-term synaptic plasticity. Cell. 118:389–401.

Lau PM, Bi GQ. 2005. Synaptic mechanisms of persistent reverberatory activity in neuronal networks. Proc Natl Acad Sci USA. 102:10333–10338.

Lazarevic V, Schone C, Heine M, Gundelfinger ED, Fejtova A. 2011. Extensive remodeling of the presynaptic cytomatrix upon homeostatic adaptation to network activity silencing. J Neurosci. 31:10189–10200.

London M, Hausser M. 2005. Dendritic computation. Annu Rev Neurosci. 28:503–532.

London M, Roth A, Beeren L, Hausser M, Latham PE. 2010. Sensitivity to perturbations in vivo implies high noise and suggests rate coding in cortex. Nature. 466:123–127.

Lou X, Korogod N, Brose N, Schneggenburger R. 2008. Phorbol esters modulate spontaneous and Ca2+-evoked transmitter release via acting on both Munc13 and protein kinase C. J Neurosci. 28:8257–8267.

Lou X, Scheuss V, Schneggenburger R. 2005. Allosteric modulation of the presynaptic Ca2+ sensor for vesicle fusion. Nature. 435:497–501.

Luck SJ, Chelazzi L, Hillyard SA, Desimone R. 1997. Neural mechanisms of spatial selective attention in areas V1, V2, and V4 of macaque visual cortex. J Neurophysiol. 77:24–42.

Malenka RC, Nicoll RA. 1999. Long-term potentiation—a decade of progress? Science. 285:1870–1874.

Marom S, Shahaf G. 2002. Development, learning and memory in large random networks of cortical neurons: lessons beyond anatomy. Q Rev Biophys. 35:63–87.

Martin TF. 2003. Tuning exocytosis for speed: fast and slow modes. Biochim Biophys Acta. 1641:157–165.

McCormick DA. 2005. Neuronal networks: flip-flops in the brain. Curr Biol. 15:R294–296.

McKinney RA, Capogna M, Durr R, Gahwiler BH, Thompson SM. 1999. Miniature synaptic events maintain dendritic spines via AMPA receptor activation. Nat Neurosci. 2:44–49.

McMahon HT, Kozlov MM, Martens S. 2010. Membrane curvature in synaptic vesicle fusion and beyond. Cell. 140:601–605.

Miller P, Wang XJ. 2006. Stability of discrete memory states to stochastic fluctuations in neuronal systems. Chaos. 16:026109.

Mochida S, Orita S, Sakaguchi G, Sasaki T, Takai Y. 1998. Role of the Doc2 alpha-Munc13-1 interaction in the neurotransmitter release process. Proc Natl Acad Sci USA. 95:11418–11422.

Otsu Y, Murphy TH. 2003. Miniature transmitter release: accident of nature or careful design? Sci STKE. 2003:pe54.

Pang ZP, Bacaj T, Yang X, Zhou P, Xu W, Sudhof TC. 2011. Doc2 supports spontaneous synaptic transmission by a Ca(2+)-independent mechanism. Neuron. 70:244–251.

Pang ZP, Sun J, Rizo J, Maximov A, Sudhof TC. 2006. Genetic analysis of synaptotagmin 2 in spontaneous and Ca2+-triggered neurotransmitter release. EMBO J. 25:2039–2050.

Pasquale V, Martinoia S, Chiappalone M. 2010. A self-adapting approach for the detection of bursts and network bursts in neuronal cultures. J Comput Neurosci. 29:213–229.

Rettig J, Neher E. 2002. Emerging roles of presynaptic proteins in Ca++-triggered exocytosis. Science. 298:781–785.

Rhee JS, Betz A, Pyott S, Reim K, Varoqueaux F, Augustin I, Hesse D, Sudhof TC, Takahashi M, Rosenmund C et al. 2002. Beta phorbol ester- and diacylglycerol-induced augmentation of transmitter release is mediated by Munc13s and not by PKCs. Cell. 108:121–133.

Ronnback A, Dahlqvist P, Svensson PA, Jernas M, Carlsson B, Carlsson LM, Olsson T. 2005. Gene expression profiling of the rat hippocampus one month after focal cerebral ischemia followed by enriched environment. Neurosci Lett. 385:173–178.

Rosenmund C, Rettig J, Brose N. 2003. Molecular mechanisms of active zone function. Curr Opin Neurobiol. 13:509–519.

Rosenmund C, Sigler A, Augustin I, Reim K, Brose N, Rhee JS. 2002. Differential control of vesicle priming and short-term plasticity by Munc13 isoforms. Neuron. 33:411–424.

Sanchez-Vives MV, McCormick DA. 2000. Cellular and network mechanisms of rhythmic recurrent activity in neocortex. Nat Neurosci. 3:1027–1034.

Sara Y, Virmani T, Deak F, Liu X, Kavalali ET. 2005. An isolated pool of vesicles recycles at rest and drives spontaneous neurotransmission. Neuron. 45:563–573.

Sharma G, Vijayaraghavan S. 2003. Modulation of presynaptic store calcium induces release of glutamate and postsynaptic firing. Neuron. 38:929–939.

Shin OH, Lu J, Rhee JS, Tomchick DR, Pang ZP, Wojcik SM, Camacho-Perez M, Brose N, Machius M, Rizo J et al. 2010. Munc13 C2B domain is an activity-dependent Ca2+ regulator of synaptic exocytosis. Nat Struct Mol Biol. 17:280–288.

Shin OH, Rhee JS, Tang J, Sugita S, Rosenmund C, Sudhof TC. 2003. Sr2+ binding to the Ca2+ binding site of the synaptotagmin 1 C2B domain triggers fast exocytosis without stimulating SNARE interactions. Neuron. 37:99–108.

Shu Y, Hasenstaub A, McCormick DA. 2003. Turning on and off recurrent balanced cortical activity. Nature. 423:288–293.

Silva AJ, Rosahl TW, Chapman PF, Marowitz Z, Friedman E, Frankland PW, Cestari V, Cioffi D, Sudhof TC, Bourtchuladze R. 1996. Impaired learning in mice with abnormal short-lived plasticity. Curr Biol. 6:1509–1518.

Stegenga J, Le Feber J, Marani E, Rutten WL. 2008. Analysis of cultured neuronal networks using intraburst firing characteristics. IEEE Trans Biomed Eng. 55:1382–1390.

Steriade M, Nunez A, Amzica F. 1993. A novel slow (<1 Hz) oscillation of neocortical neurons in vivo: depolarizing and hyperpolarizing components. J Neurosci. 13:3252–3265.

Stevenson IH, Rebesco JM, Miller LE, Kording KP. 2008. Inferring functional connections between neurons. Curr Opin Neurobiol. 18:582–588.

Sun J, Pang ZP, Qin D, Fahim AT, Adachi R, Sudhof TC. 2007. A dual-Ca2+-sensor model for neurotransmitter release in a central synapse. Nature. 450:676–682.

Timofeev I, Grenier F, Bazhenov M, Sejnowski TJ, Steriade M. 2000. Origin of slow cortical oscillations in deafferented cortical slabs. Cereb Cortex. 10:1185–1199.

Timofeev I, Grenier F, Steriade M. 2001. Disfacilitation and active inhibition in the neocortex during the natural sleep-wake cycle: an intracellular study. Proc Natl Acad Sci USA. 98:1924–1929.

Tokumaru H, Augustine GJ. 1999. UNC-13 and neurotransmitter release. Nat Neurosci. 2:929–930.

Toscano CD, McGlothan JL, Guilarte TR. 2006. Experience-dependent regulation of zif268 gene expression and spatial learning. Exp Neurol. 200:209–215.

Van Pelt J, Corner MA, Wolters PS, Rutten WL, Ramakers GJ. 2004. Longterm stability and developmental changes in spontaneous network burst firing patterns in dissociated rat cerebral cortex cell cultures on multielectrode arrays. Neurosci Lett. 361:86–89.

Wagenaar DA, Pine J, Potter SM. 2006. An extremely rich repertoire of bursting patterns during the development of cortical cultures. BMC Neurosci. 7:11.

Wang XJ, Buzsaki G. 1996. Gamma oscillation by synaptic inhibition in a hippocampal interneuronal network model. J Neurosci. 16:6402–6413.

Weihberger O, Okujeni S, Mikkonen JE, Egert U. 2012. Quantitative examination of stimulus-response relations in cortical networks in vitro. J Neurophysiol. In press.

Weimer RM, Gracheva EO, Meyrignac O, Miller KG, Richmond JE, Bessereau JL. 2006. UNC-13 and UNC-10/rim localize synaptic vesicles to specific membrane domains. J Neurosci. 26: 8040–8047.

Xu W, Morishita W, Buckmaster PS, Pang ZP, Malenka RC, Sudhof TC. 2012. Distinct neuronal coding schemes in memory revealed by selective erasure of fast synchronous synaptic transmission. Neuron. 73:990–1001.

Xu-Friedman MA, Regehr WG. 1999. Presynaptic strontium dynamics and synaptic transmission. Biophys J. 76:2029–2042.

Xu-Friedman MA, Regehr WG. 2000. Probing fundamental aspects of synaptic transmission with strontium. J Neurosci. 20:4414–4422.

Yao J, Gaffaney JD, Kwon SE, Chapman ER. 2011. Doc2 is a ca(2+) sensor required for asynchronous neurotransmitter release. Cell. 147:666–677.